Available online at www.sciencedirect.com

ScienceDirect

journal homepage: www.JournalofSurgicalResearch.com

Use of a pedicled omental flap to reduce inflammation and vascularize an abdominal wall patch

Takafumi Uchibori,[a,b,c] *Keisuke Takanari,*[a,b,c] *Ryotaro Hashizume,*[a,b] *Nicholas J. Amoroso,*[a,d] *Yuzuru Kamei,*[c] *and William R. Wagner*[a,b,d,*]

[a] *McGowan Institute for Regenerative Medicine, University of Pittsburgh*
[b] *Department of Surgery, University of Pittsburgh*
[c] *Department of Plastic and Reconstructive Surgery, Nagoya University Graduate School of Medicine, Nagoya, Japan*
[d] *Department of Bioengineering, University of Pittsburgh, Pittsburgh, Pennsylvania*

ARTICLE INFO

Article history:
Received 23 August 2016
Received in revised form
23 November 2016
Accepted 29 November 2016
Available online xxx

Keywords:
Omental flap
Biodegradable patch
Macrophage
Inflammation
Vascularization
Abdominal wall

ABSTRACT

Background: Although a variety of synthetic materials have been used to reconstruct tissue defects, these materials are associated with complications such as seromas, fistulas, chronic patient discomfort, and surgical site infection. While alternative, degradable materials that facilitate tissue growth have been examined. These materials can still trigger a foreign body inflammatory response that can lead to complications and discomfort.

Materials and methods: In this report, our objective was to determine the effect of placing a pedicled omental flap under a biodegradable, microfibrous polyurethane scaffold serving as a full-wall thickness replacement of the rat abdominal wall. It was hypothesized that the presence of the omental tissue would stimulate greater vascularization of the scaffold and act to reduce markers of elevated inflammation in the patch vicinity. For control purposes, a polydimethylsiloxane sheet was placed as a barrier between the omental tissue and the overlying microfibrous scaffold. Both groups were sacrificed 8 wk after the implantation, and immunohistological and RT-PCR assessments were performed.

Results: The data showed omental tissue placement to be associated with increased vascularization, a greater local M2/M1 macrophage phenotype response, and mRNA levels reduced for inflammatory markers but increased for angiogenic and antiinflammatory factors.

Conclusions: From a clinical perspective, the familiarity with utilizing omental flaps for an improved healing response and infection resistance should naturally be considered as new tissue engineering approaches that are translated to tissue beds where omental flap application is practical. This report provides data in support of this concept in a small animal model.

* *Corresponding author.* McGowan Institute for Regenerative Medicine, Department of Bioengineering, University of Pittsburgh, Pittsburgh, PA. Tel.: +1 412-624-5324; fax: +1 412-624-5363.
E-mail address: wagnerwr@upmc.edu (W.R. Wagner).

0022-4804/$ – see front matter © 2016 Elsevier Inc. All rights reserved.
http://dx.doi.org/10.1016/j.jss.2016.11.052

Introduction

In clinical practice, autologous fascia lata or synthetic materials, including polypropylene and polyester meshes, and expanded polytetrafluoroethylene, are mainly used to repair or reinforce tissue defects.[1] However, the use of such materials can be associated with complications such as seromas, fistulas, chronic patient discomfort, and surgical site infection.[2-5] To circumvent these issues, researchers have been devising operative procedures or developing materials that have increased resistance to infection and better functional outcomes. Biodegradable synthetic materials designed to facilitate tissue ingrowth and scaffold remodeling and that result in tissues which mechanically approximate native tissue would represent a regenerative approach likely to reduce the complications seen with current replacement materials.

Recent reports have shown the repair of abdominal wall defects in a small animal model utilizing a microfibrillar, biodegradable poly (ester urethane) urea (PEUU) generated with electrospinning techniques. The data suggest that this approach might provide sufficient strength along with cellular infiltration.[6-8] Although the tissue response to the PEUU material appeared adequate, at least in an acute model, one might wish to achieve a biological response with greater vascularization and the potential for greater infection resistance. It is known that the placement of an omental tissue flap near artificial implanted surfaces provides some protection against infection and stimulates wound healing, particularly in terms of vascularization. This technique is often used clinically in inflammatory situations including pyothorax and osteomyelitis or to control infection risk from artificial materials such as expanded polytetrafluoroethylene and materials serving as skull plates and vascular grafts.[9-12] In tissue engineering, omentum has been used as an *in situ* bioreactor and to improve local angiogenesis in response to scaffold implants.[13-20] In this report, our objective was to determine the effect of placing a pedicled omental flap under a biodegradable, microfibrous PEUU scaffold serving as a full wall thickness replacement of the rat abdominal wall. It was hypothesized that the presence of the omental tissue would stimulate greater vascularization of the scaffold and act to reduce markers of elevated inflammation in the patch vicinity. For control purposes, a polydimethylsiloxane (silicone) sheet was placed as a barrier between the omental tissue and the overlying microfibrous PEUU scaffold.

Materials and methods

Scaffold fabrication

PEUU was synthesized from polycaprolactone diol (Mn = 2000), 1,4-diisocyanatobutane (Sigma–Aldrich, St. Louis, MO), and putrescine (Sigma-Aldrich), according to previously described methods.[8] For this study, a wet electrospun PEUU (wet ePEUU) scaffold was made by concurrently electrospinning the polymer and electrospraying culture medium. The cell culture medium employed was Dulbecco's modified Eagle medium (DMEM, Invitrogen, Carlsbad, CA) with 10% fetal bovine serum (GIBCO, Grand Island, NY), 10% horse serum (GIBCO), 1% penicillin/streptomycin (GIBCO), and 0.5% chick embryo extract (GIBCO). The culture medium was contained in a syringe with a 1.2-mm inner diameter steel capillary attached and placed in a syringe pump. The capillary was charged at 7 kV and suspended 4 cm above a 6-mm diameter mandrel. Medium flow through the capillary was 0.2 mL/min. At the same time, PEUU dissolved in hexafluoroisopropanol (12%, w/v) was placed in a syringe with an attached steel capillary and placed 20 cm from the mandrel, perpendicular to the medium-containing syringe. A syringe pump was used to flow the polymer solution at 1.5 mL/h with the capillary charged at 12 kV. The mandrel was charged at −4 kV and rotated at 250 rpm (8-cm/s tangential velocity) while translating back and forth 8 cm along the x-axis at 0.15 cm/s (Fig. 1B).

Animal model

Adult, female syngeneic Lewis rats (Harlan Laboratories, Indianapolis, IN) aged 10- to 12-weeks old and weighing 200-250g were used for this procedure. This gender and age was selected since the growth curve for female Lewis rats plateaus earlier than male rats, and the created surgical defects would not be affected by the ongoing growth expected with the male rats. A single gender was utilized to minimize the effect of different growth rates on the healing response. The Institutional Animal Care and Use Committee of the University of Pittsburgh approved the procedure protocols. Anesthesia was achieved by inhalation of 1.25%-2.5% isoflurane with 100% oxygen. The abdomen was sterilized with povidone-iodine solution, and procedures were performed in a sterile environment on a heating blanket. The surgical procedure was based on that previously reported by Hashizume *et al.*[8]

A skin incision was made above the linea alba 3.5 cm in length from 2 cm caudal of the xiphoid process. A surgical defect (1 × 2.5 cm) included all the layers of the abdominal wall including the fascia, rectus abdominis muscle, and parietal peritoneum, but the skin and subcutaneous soft tissue were preserved. This anatomical defect was then repaired with the generated scaffolds sutured to a pedicled omental flap or to a sterilized silicon sheet (4 × 6 cm size, 0.02-cm thick, BioPlexus, CA). The pedicled omental flap was prepared by detachment from the transverse colon and spread on the bowel (Fig. 1A). The scaffolds (1 × 2.5 cm, 400-μm thick) were sutured to the peripheral abdominal fascia and muscle with a continuous 7-0 polypropylene suture without overlap between muscle and scaffold and in direct contact with the subcutaneous tissue and the bowels. Skin closure over the patch was achieved by double-layer suturing. For postoperative analgesic treatment, 0.1-mg/kg buprenorphine and 100-mg/kg cefuroxime were injected subcutaneously twice daily for 3 days after procedure.

For the omental-attached (omentum) group, the implanted samples were surgically retrieved at 4 and 8 wk postimplantation ($n = 7$ per time point). For the silicon barrier (control) group, implanted samples were retrieved 8 wk postimplantation ($n = 7$). At retrieval, animals were euthanized by 5% isoflurane inhalation, and the abdominal wall was circumferentially incised to expose the peritoneal cavity and

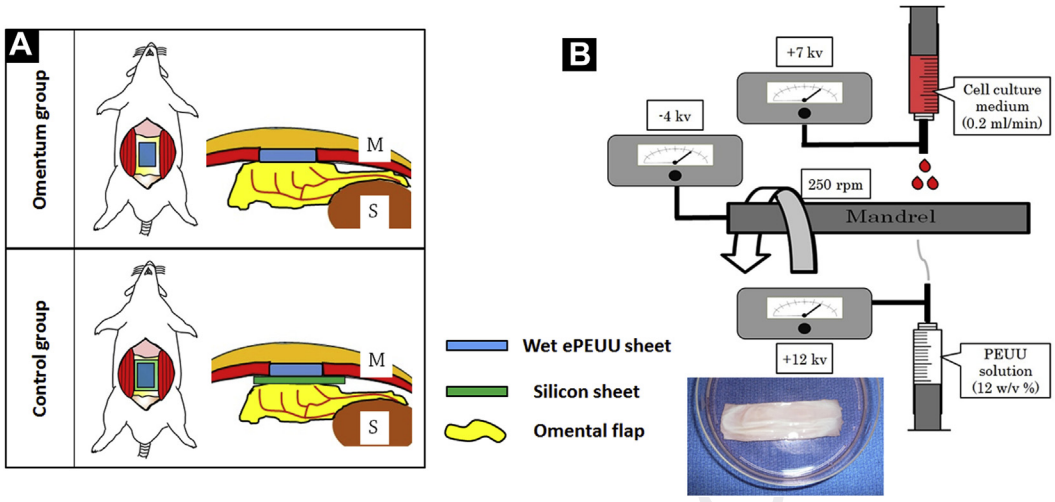

Fig. 1 – Surgical procedure. (A) A wet electrospun PEUU scaffold was fabricated by the concurrent polymer electrospinning and culture medium electrospraying. Lower image is material detached from the mandrel. (B) A 2.5 × 1 cm abdominal wall defect was created and repaired with PEUU scaffolds on pedicled omental flap (omentum group) or silicon sheet (control group). M = abdominal muscle; S = stomach. (Color version of figure is available online.)

the repair site. Representative specimens were photographed *in situ* for later review and comparisons. The patches were explanted by cutting with approximately a 5-mm margin from the original suture line and divided for histology, immunohistochemistry, and RT-PCR.

Histology and immunohistochemistry

For hematoxylin and eosin and Masson's trichrome staining, the samples were fixed in 10% formalin solution for 24 h, embedded in paraffin, sectioned into 8-μm thick specimens, and stained. For immunohistology, samples were fixed in 4% phosphate-buffered paraformaldehyde for 2 h, immersed in 30% sucrose for 48 h, frozen, and cryosectioned into 8-μm thick specimens. Sections for immunohistochemistry were reacted with primary antibodies. The primary antibodies used for immunohistochemical staining were mouse anti-rat CD163 (Serotec, Oxford, UK) at 1:100 dilution, rabbit anti-CCR7 (Abcam, Cambridge, UK) at 1:800 dilution, rabbit anti-rat von Willebrand factor (vWF; Abcam) at 1:1000 dilution, and mouse anti-rat alpha smooth muscle actin (Abcam) at 1:200 dilution. The slides were counterstained with DAPI (IHC World, Ellicott City, MD). For each sample retrieved, 10 different microscopic fields were photographed for CD163-, CCR7-, vWF-, and alpha smooth muscle actin–positive structures at 200 × magnification and quantified using IMAGE J software, (National Institutes of Health, Bethesda, MD). Capillaries were identified as tubular structures positively stained for vWF.

RT-PCR

Retrieved samples were immediately immersed in liquid nitrogen and stored in a −80°C freezer until analysis. For RNA extraction, areas of the retrieved samples were chopped in small pieces, and approximately, 30 mg was processed as previously described.[8] Briefly, total RNA was extracted from the retrieved tissues using an RNeasy Mini Kit (Qiagen, Venlo, Netherlands). Complementary DNA (cDNA) was synthesized with RNA to cDNA EcoDry Premix reverse transcriptase (Clonetech, Mountain View, CA, USA), according to the manufacturer's instructions. cDNAs and primers were added to SYBR Green PCR master mix (Applied Biosystems, Foster City, CA), according to the manufacturer's instructions. Quantitative analysis was then performed with primers (Real Time Primers, Elkins Park, PA). All data were normalized to beta-actin, which was used as an internal control, and further by expression relative to the control group. The sequences, amplicon positions, and gene accession numbers of the primers used for PCR are listed in the Table (Table).

Statistical analyses

Statistical analyses were performed using IBM SPSS Statistics 22 (IBM, Armonk, NY). Results are presented as mean ± standard deviation. Differences were considered to be statistically significant at $P < 0.05$. In this study, the 8-wk omentum group was compared with the 8-wk control group and with the 4-wk omentum group respectively. One-way analysis of variance was used with Bonferroni post hoc testing.

Results

Macroscopic observations

The omentum group had a muscle border that showed evidence of integration and was surrounded by blood vessels and abdominal wall muscle. Qualitative comparisons with the control group at 8 wk suggested more surface vascularization and a smoother transition to the peripheral muscle (Fig. 2A). The wall thickness for both groups increased significantly from preimplantation to the 8 wk time point, with no differences between the omentum and control groups (Fig. 2C). No herniation was observed in either group.

Table – DNA sequences of the primers.

Gene	Sequence information
β-actin	
Forward	5′-CAC ACT GTG CCC ATC TAT GA-3′
Reverse	5′-CCG ATA GTG ATG ACC TGA CC-3′
VEGF	
Forward	5′-TCA CAG GGA GAA GAG TGG AG-3′
Reverse	5′-AGC CAG AAG ATG CTC ACT TG-3
IL-10	
Forward	5′-GAC GCT GTC ATC GAT TTC TC-3′
Reverse	5′-TTC ATG GCC TTG TAG ACA CC-3′
IL-1ra	
Forward	5′-AAG ACC TTC TAC CTG AGG AAC AACC-3′
Reverse	5′-GCC CAA GAA CAC ATT CCG AAA GTC-3′
IL-1β	
Forward	5′-AGA GTG TGG ATC CCA AAC AA-3′
Reverse	5′-AGT CAA CTA TGT CCC GAC CA-3′
IL-12	
Forward	5′-TGC AGA GAA GGT CAC ACT GA-3′
Reverse	5′-GAT GAA GAA GCT GGT GCT GT-3′

Histological assessment

Histological assessment showed that both groups had extensive cellular infiltration at both time points, and the omentum group showed much more blood vessels than the control group at higher magnification (Fig. 3). Vascular ingrowth was observed in both scaffold types at both time points. However, the number of blood vessels was greater in the omentum group than that in the control group at 8 wk (48 ± 15 vs 27 ± 7). The number of foreign body giant cells (FBGCs) was greater in the control group than that in the omentum group (17 ± 4 vs 10 ± 2; Fig. 4).

Immunohistochemical assessment

Assessment of scaffold site remodeling with immunostaining for macrophage phenotype showed that the ratio of CD163-positive cells (characteristic of M2 macrophages) to CCR7-positive cells (characteristic of M1 macrophages) increased for the omentum group and was greater at 8 wk than that at 4 wk (Fig. 5). Macrophages consistent with the M2 phenotype appeared to infiltrate the patches from the abdominal (omental placed) side. The images in Figure 5 were taken from scaffold sections where the omental flap had been detached from the lower side of the scaffolds. Vascular density within the patches, as assessed by vWF immunostaining, showed that the omentum group had greater vascularization than the control group, and this difference increased for the omentum group from 4 to 8 wk. The vWF positive structures were often surrounded by α-smooth muscle actin-positive cells (Fig. 6). In examining the border between the scaffold and omental tissue at 8 wk, there was evidence of continuity between the omental tissue and the scaffold materials with closely positioned vasculature and M2 macrophages (Fig. 7). Unlike the image from Figure 5, the omental tissue remained attached to the scaffold before sectioning for Figure 7.

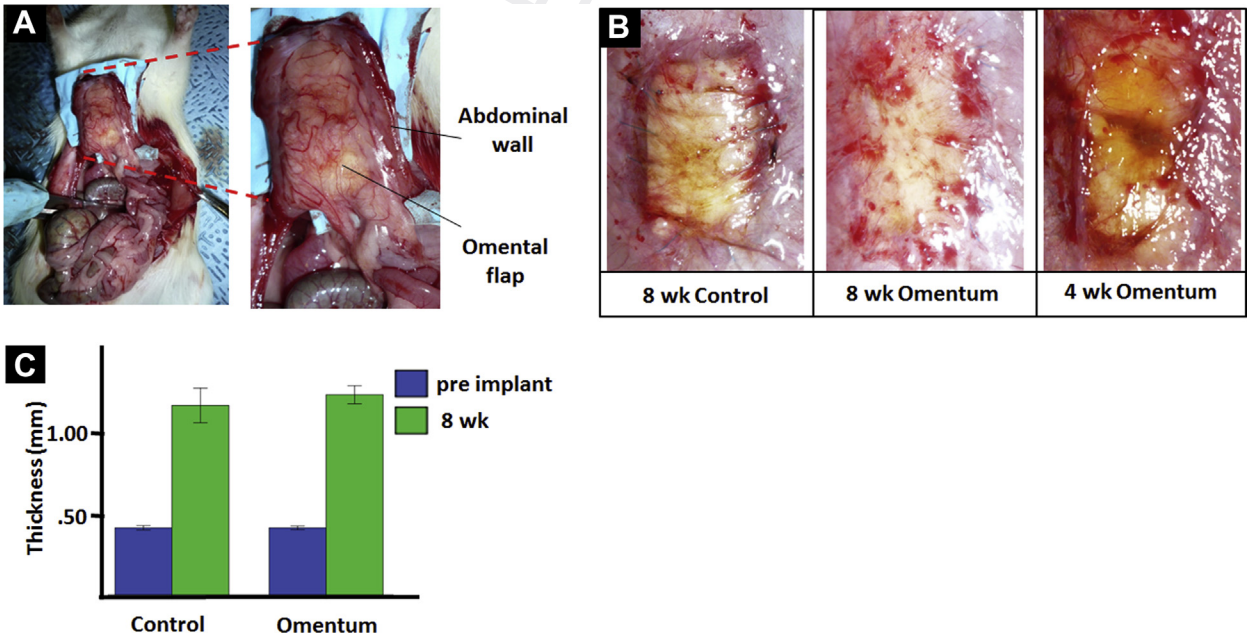

Fig. 2 – Observations at explant. (A) At explant, the omental flap was well adhered to the material. (B) In the omentum group, the scaffold was surrounded by blood vessels and appeared to be better integrated with the abdominal wall in contrast to the control group. (C) The wall thickness for both groups increased significantly from preimplantation to the 8 wk time point, with no differences between the groups. Error bars = ± standard deviation. (Color version of figure is available online.)

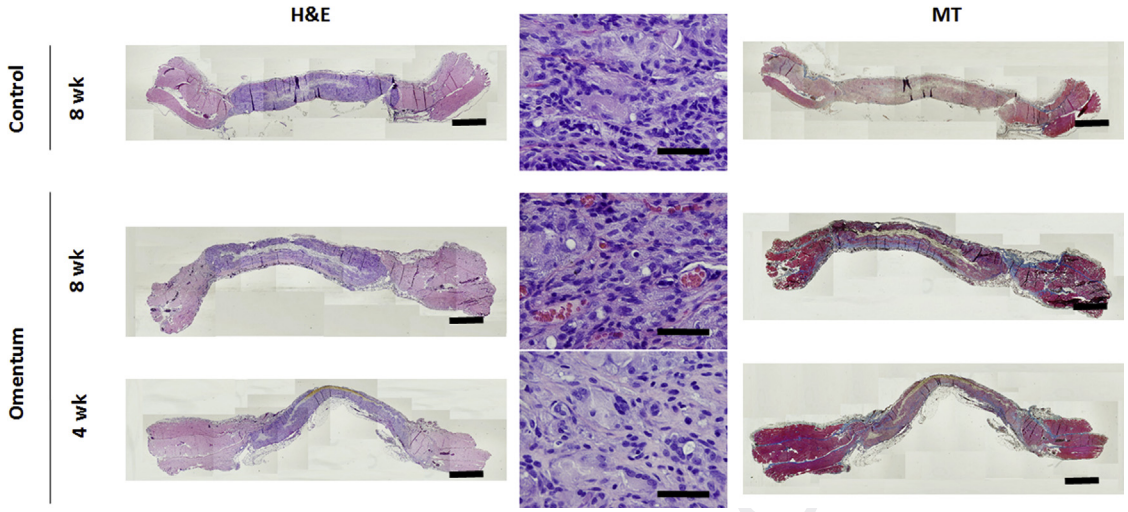

Fig. 3 – Histology. Representative cross section of implanted scaffold at 4 and 8 wk after implantation. Both scaffold types had extensive cellular infiltration at both time points. High magnification images are shown. 8-wk groups had more cells, and the omentum groups had more blood vessels. Scale bars = 1 mm and 100μm (center images). H and E = hematoxylin and eosin; MT = Masson's trichrome. (Color version of figure is available online.)

RT-PCR

Assessment of RNA expression showed that at 8 wk, the omentum group had greater VEGF and IL-1 receptor antagonist expression than the control group, and a similar amount of IL-10 expression. The expression of IL-12 and IL-1 was lower in the omentum group (Fig. 8).

Discussion

The use of synthetic materials to support or replace soft tissue deficits leads to a foreign body response, characterized ultimately by the formation of fibrous tissue around the implanted material. In many cases, this response is acceptable,

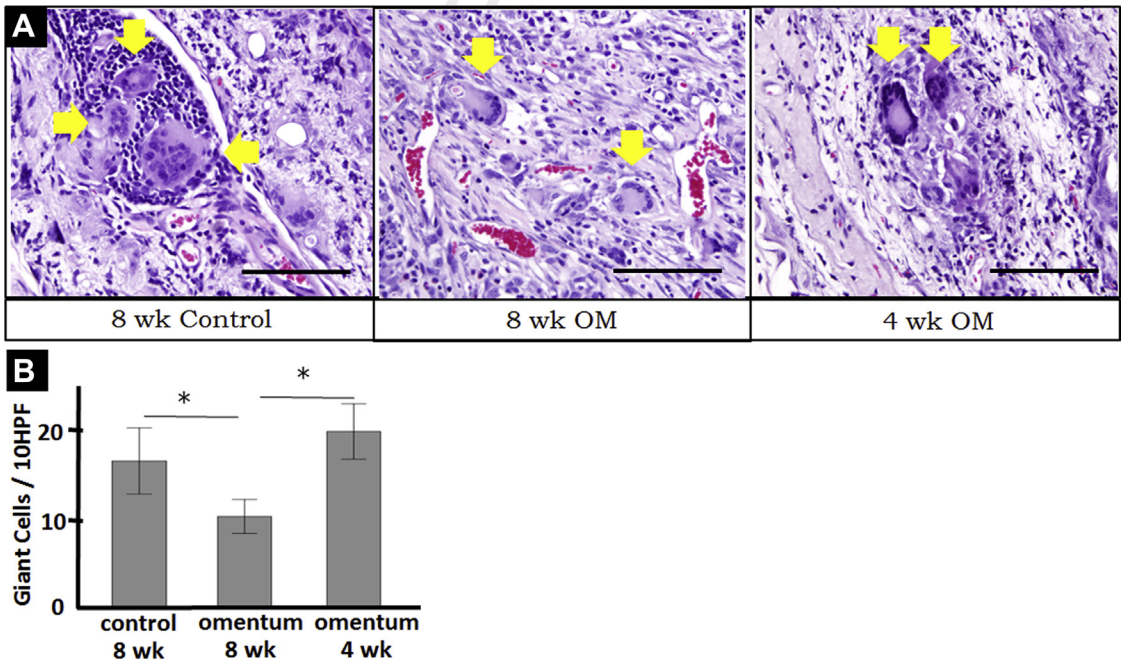

Fig. 4 – Foreign body giant cells. (A) High magnification images of the samples (HE). Giant cells could be seen in all groups (yellow arrows). Scale bars = 100 μm. (B) The number of the giant cells shown as mean number ± standard deviation (10 high power fields/rat with 7 rats/group). The omentum group had lower numbers of giant cells in the explants at 8 wk *versus* control, but this number was reduced *versus* the 4 wk omentum group. (*P < 0.05). (Color version of figure is available online.)

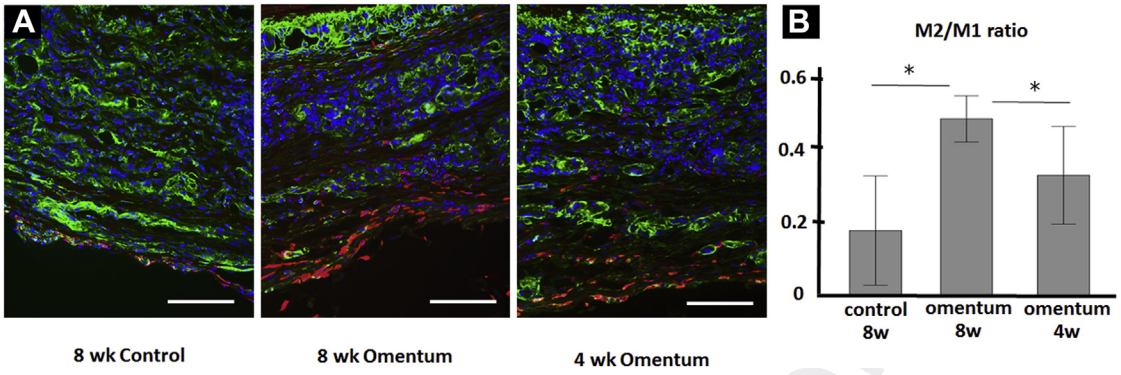

Fig. 5 – Macrophage type. (A) Immunostaining for type 1 macrophages (CCR7, M1; green), type 2 macrophages (CD163, M2; red), and Hoechst (blue) for samples from the omentum (4 and 8 wk) and control groups. Scale bars = 100 μm. (B) Quantitative image analysis of the M1 and M2 stained areas. The omentum group had a greater M2/M1 ratio compared to the control group at the 8 wk time point (*P < 0.05). Error bars = ± standard deviation. (Color version of figure is available online.)

although nonideal. Of more concern are complications such as biomaterial-centered infections, chronic inflammation, and host responses that can lead to mechanical failure of the implant or stress concentrations at the interface between a stiff implant and more compliant host tissue. To address some of these complications, the placement of muscle, cutaneous, and omental flaps have been used, in some cases prophylactically, but often as a strategy to avoid device removal. The movement of viable and well-vascularized tissue to the implant region can effectively improve the biocompatibility of the artificial materials by altering some aspects of the local tissue response.

The provision of a source for vascular ingrowth is one hypothesized benefit of local flap placement, but the specific mechanisms by which flap placement provides benefit are not well defined. In the context of placement of greater omental flaps, some reports show that the flap facilitates angiogenesis in a similar manner as other flaps, resulting in control of infection and good tissue remodeling.[13-18] Other reports indicate that the omental flap controls not only angiogenesis but also provides protection against infection and inflammatory reactions.[19,20] The beneficial antiinflammatory effect may be attributable to the cellular components and cytokines derived from the omental flap.[21,22] Although omental flaps have been used to improve the local physiological response to artificial materials in many studies, few reports examine the mechanisms for an improved response in the setting of biomaterial placement.

According to the results from immunohistochemistry and PCR in this study, angiogenesis was significantly facilitated in the omentum group compared with the control group. In considering the local macrophage population, the M2/M1 ratio was markedly higher in the omentum group than that in the control group, and numerous M2 macrophages accumulated near the omental side of the scaffold implant, whereas M1 macrophages accumulated around the material in the omentum group (Figs. 5 and 7B). In the control group, almost no M2 macrophages were observed on the abdominal side, although some were observed on the skin side. The M1 phenotype is generally associated with the classic foreign body response, whereas the M2 phenotype near biomaterial implants has been associated with constructive remodeling, an increased M2 population may be desirable for tissue regeneration.[23,24] The local omental tissue may facilitate M2

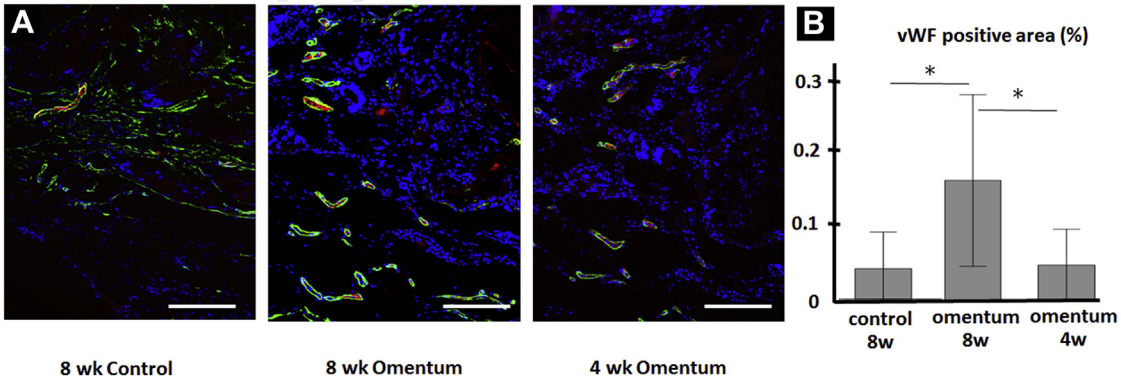

Fig. 6 – Vascularization. (A) Immunostaining for von Willebrand factor (vWF; red), alpha smooth muscle actin (SMA; green), and Hoechst (blue) for samples from the omentum (4 and 8 wk) and control groups. Scale bars = 100 μm. (B) Quantitative image analysis of the vWF-stained area. At 8 wk, the omentum group had greater vWF positively stained areas compared to the control group (*P < 0.05). Error bars = ± standard deviation. (Color version of figure is available online.)

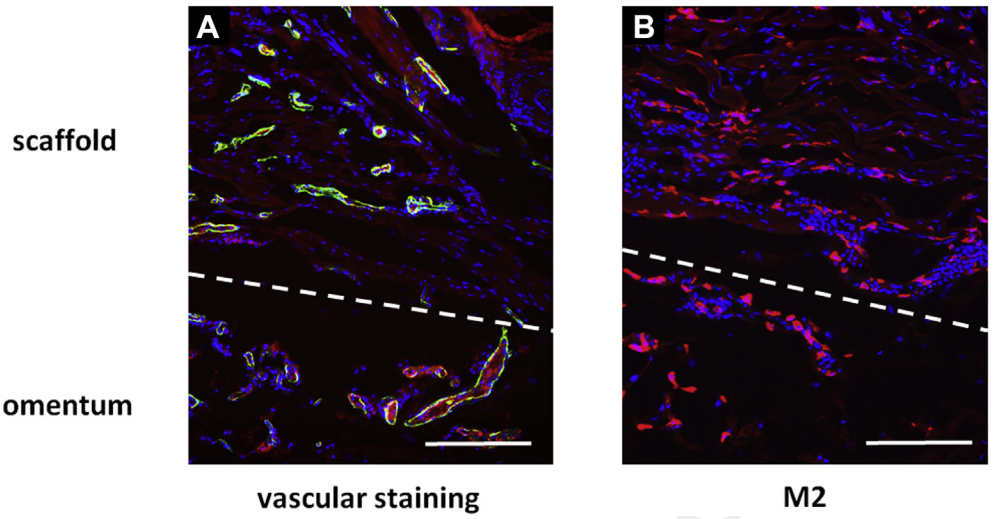

Fig. 7 – Border between scaffold and omentum. (A) Immunostaining for von Willebrand factor (vWF; red), alpha-smooth muscle actin (SMA; green), and Hoechst (blue) for samples from the omentum 8-wk group. Scale bars = 100 μm. (B) Immunostaining for type 2 macrophages (CD163, M2; red) and Hoechst (blue) for samples from the omentum 8 wk group. Scale bars = 100 μm. (Color version of figure is available online.)

expression, and this function may be associated with the antiinflammatory effect of the greater omentum itself. Some angiogenic cytokines are released by M1 macrophages, which are also reportedly involved in angiogenesis, but the involvement of M2 macrophages is considered to be more substantial in this process.[25] The ratio of M2/M1 in this study was higher at 8 wk than that at 4 wk, and this was consistent with a previous study in a similar animal model, which showed that the proportion of M2 macrophages increased progressively from 4 wk to 8 wk, although the used material was slightly different, and omental tissue placement was not employed.[26] FBGC formation, which is a common response to synthetic material implantation, is considered to be associated to type 1 macrophage action and is often seen at the chronic inflammatory stage.[27] At the 8 wk time point, the number of FBGCs was significantly less for the omentum group, consistent with a moderated foreign body response and reduced M1 activity. To our knowledge, this is the first report that has examined

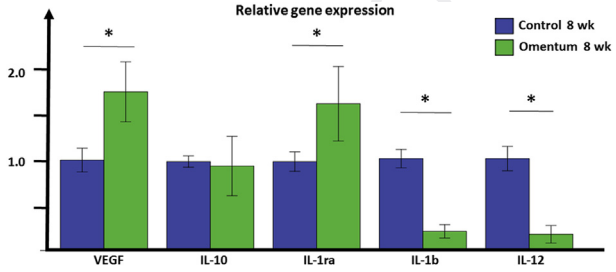

Fig. 8 – RT-PCR: RT-PCR results from the scaffold region for VEGF, IL-10, IL-1 receptor antagonist, IL-1b, and IL-12. The values for the omentum group were normalized by beta-actin, and further normalized by the value of the control group at the 8-wk time point. Data are shown as relative expression compared to the control group (*$P < 0.05$). Error bars = ± standard deviation. (Color version of figure is available online.)

the effect of omental tissue placement on the M2 macrophage response to a foreign body implantation.

Consistent with the M2 and M1 macrophage response discussed previously, there was evidence of a decrease in local inflammatory cytokines with omental tissue placement and an increase in IL-1ra. These mRNA data were accompanied by a significant increase in VEGF mRNA. These data, together with the macrophage phenotype data support the earlier suggestion that both cellular and humoral actions associated with local omental tissue are acting to improve local angiogenesis and modulate the foreign body response. In the future, a broader array of factors involved in inflammatory pathways could be investigated in greater detail. Also, the macrophage markers employed in this report were limited to CCR7 and CD163. CD86, CD206, CD68, and other phenotype-specific markers could be used to characterize M1 and M2 cells in greater detail. Another limitation was the investigation of only two time points, 4 and 8 wk. Although at 8 wk, the omentum group showed several indicators consistent with a moderated inflammatory reaction relative to the control group, it may not be enough to definitively support a positive role for the omentum in regulating the foreign body response in this model Longer time points would add important insight into where the local response ultimately stabilizes, and additional early time points for the control and omentum groups would better define the relative benefit for omental tissue in this early period, where the limited data of this report may indicate less of a clear benefit. Finally, the rodent model is clearly limited in terms of extrapolation to the clinical setting. In particular, the areas and volumes of material being implanted may mitigate some of the benefits of a closely placed omental flap. Although this study used a silicone sheet as a barrier between the omental tissue and the overlying scaffold to isolate the effect of intentionally placed omental tissue, in the absence of such a barrier, some variable omental tissue adhesion may be expected to occur and bring some local benefit.

Conclusions

In reconstructing a full thickness abdominal wall defect in the rat, placing a pedicled omental flap under a biodegradable, microfibrous elastomeric scaffold was associated with greater vascularization of the scaffold and a reduction in the inflammatory markers that are characteristic of the foreign body response. The reduced response was characterized with respect to the control surgery, where a polydimethylsiloxane sheet was placed as a barrier between the omental tissue and the overlying microfibrous scaffold. These results have implications for the use of this approach beyond the use of materials in abdominal wall reconstruction but also for other tissue defects where a combined temporary scaffold and omental flap approach might be employed. From a clinical perspective, the familiarity with using omental flaps for an improved healing response and infection resistance should naturally be considered as new tissue engineering approaches are translated to tissue beds where omental flap application is practical.

Acknowledgment

This work was supported in part by the Armed Forces Institute of Regenerative Medicine (AFIRM, #W81XWH-08-2-0032, W81XWH-14-2-0004). The authors would also like to thank Deanna Rhoads for histological sectioning and the Center for Biological Imaging at the University of Pittsburgh for assistance in imaging.

Author contributions: T.U., K.T., W.R.W., and Y.K. were responsible for the study conception and design. T.U., R.H., and N.J.A. contributed to the data collection. T.U. and K.T. analyzed and interpreted the data. T.U. and W.R.W. prepared the manuscript.

Disclosure

The authors reported no proprietary or commercial interest in any product mentioned or concept discussed in the article.

REFERENCES

1. Campanelli G, Catena F, Ansaloni L. Prosthetic abdominal wall hernia repair in emergency surgery: from polypropylene to biological meshes. *World J Emerg Surg*. 2008;3:33.
2. Candage R, Jones K, Luchette FA, Sinacore JM, Vandevender D, Reed 2nd RL. Use of human acellular dermal matrix for hernia repair: friend or foe? *Surgery*. 2008;144:703–709.
3. Sriussadaporn S, Sriussadaporn S, Kritayakirana K, Pak-art R. Operative management of small bowel fistulae associated with open abdomen. *Asian J Surg*. 2006;29:1–7.
4. O'Dwyer PJ, Kingsnorth AN, Molloy RG, Small PK, Lammers B, Horeyseck G. Randomized clinical trial assessing impact of a lightweight or heavyweight mesh on chronic pain after inguinal hernia repair. *Br J Surg*. 2005;92:166–170.
5. Jernigan TW, Fabian TC, Croce MA, et al. Staged management of giant abdominal wall defects: acute and long-term results. *Ann Surg*. 2003;238:349–355.
6. Hong Y, Takanari K, Amoroso NJ, et al. An elastomeric patch electrospun from a blended solution of dermal extracellular matrix and biodegradable polyurethane for rat abdominal wall repair. *Tissue Eng C Methods*. 2012;18:122–132.
7. Hong Y, Huber A, Takanari K, et al. Mechanical properties and in vivo behavior of a biodegradable synthetic polymer microfiber-extracellular matrix hydrogel biohybrid scaffold. *Biomaterials*. 2011;32:3387–3394.
8. Hashizume R, Fujimoto KL, Hong Y, et al. Morphological and mechanical characteristics of the reconstructed rat abdominal wall following use of a wet electrospun biodegradable polyurethane elastomer scaffold. *Biomaterials*. 2010;31:3253–3265.
9. Molnar TF. Current surgical treatment of thoracic empyema in adults. *Eur J Cardiothorac Surg*. 2007;32:422–430.
10. Gooden MA, Gentile AT, Mills JL, et al. Free tissue transfer to extend the limits of limb salvage for lower extremity tissue loss. *Am J Surg*. 1997;174:644–648.
11. Asai S, Kamei Y, Torii S. One-stage reconstruction of infected cranial defects using a titanium mesh plate enclosed in an omental flap. *Ann Plast Surg*. 2004;52:144–147.
12. Shah S, Sinno S, Vandevender D, Schwartz J. Management of thoracic aortic graft infections with the omental flap. *Ann Plast Surg*. 2013;70:680–683.
13. Baumert H, Simon P, Hekmati M, et al. Development of a seeded scaffold in the great omentum: feasibility of an in vivo bioreactor for bladder tissue engineering. *Eur Urol*. 2007;52:884–890.
14. Kim JH, Kim J, Kong WH, Seo SW. Factors affecting tissue culture and transplantation using omentum. *ASAIO J*. 2010;56:349–355.
15. Atala A, Bauer SB, Soker S, Yoo JJ, Retik AB. Tissue-engineered autologous bladders for patients needing cystoplasty. *Lancet*. 2006;367:1241–1246.
16. Dvir T, Kedem A, Ruvinov E, et al. Prevascularization of cardiac patch on the omentum improves its therapeutic outcome. *Proc Natl Acad Sci U S A*. 2009;1:14990–14995.
17. Zhang YG, Huang JH, Hu XY, Sheng QS, Zhao W, Luo ZJ. Omentum-wrapped scaffold with longitudinally oriented micro-channels promotes axonal regeneration and motor functional recovery in rats. *PLoS One*. 2011;6:e29184.
18. Shudo Y, Miyagawa S, Fukushima S, et al. Novel regenerative therapy using cell-sheet covered with omentum flap delivers a huge number of cells in a porcine myocardial infarction model. *J Thorac Cardiovasc Surg*. 2011;142:1188–1196.
19. Hamaji M, Kojima F, Koyasu S, et al. Development of a composite and vascularized tracheal scaffold in the omentum for in situ tissue engineering: a canine model. *Interact Cardiovasc Thorac Surg*. 2014;19:357–362.
20. Hoogenkamp HR, Koens MJ, Geutjes PJ, et al. Seamless vascularized large-diameter tubular collagen scaffolds reinforced with polymer knittings for esophageal regenerative medicine. *Tissue Eng Part C Methods*. 2011;142:1188–1196.
21. Shah S, Lowery E, Braun RK, et al. Cellular basis of tissue regeneration by omentum. *PLoS One*. 2012;7:e38368.
22. Chandra A, Srivastava RK, Kashyap MP, Kumar R, Srivastava RN, Pant AB. The anti-inflammatory and antibacterial basis of human omental defense: selective expression of cytokines and antimicrobial peptides. *PLoS One*. 2011;6:e20446.
23. Kou PM, Babensee JE. Macrophage and dendritic cell phenotypic diversity in the context of biomaterials. *J Biomed Mater Res A*. 2011;96:239–260.
24. Wolf MT, Dearth CL, Ranallo CA, et al. Macrophage polarization in response to ECM coated polypropylene mesh. *Biomaterials*. 2014;35:6838–6849.

25. Spiller KL, Anfang RR, Spiller KJ, et al. The role of macrophage phenotype in vascularization of tissue engineering scaffolds. *Biomaterials*. 2014;35:4477–4488.
26. Takanari K, Hong Y, Hashizume R, et al. Abdominal wall reconstruction by a regionally distinct biocomposite of extracellular matrix digest and a biodegradable elastomer. *J Tissue Eng Regen Med*. 2016;10:748–761.
27. Sheikh Z, Brooks PJ, Barzilay O, Fine N, Glogauer M. Macrophages, foreign body giant cells and their response to implantable biomaterials. *Materials*. 2015;8:5671–5701. Q2